

## ELEVATED CO<sub>2</sub> INDUCES DOWN-REGULATION OF PHOTOSYNTHESIS AND ALLEVIATES THE EFFECT OF WATER DEFICIT IN *Ceiba pentandra* (MALVACEAE)

Alexandra Maria Ferreira Silveira<sup>2</sup>  and Ricardo Antonio Marengo<sup>3\*</sup> 

<sup>1</sup> Received on 08.08.2022 accepted for publication on 07.08.2023.

<sup>2</sup> Instituto Nacional de Pesquisas da Amazônia, Programa de Pós-Graduação em Agricultura no Trópico Úmido, Manaus, AM - Brasil. E-mail: <bio.alfaia@gmail.com>.

<sup>3</sup> Instituto Nacional de Pesquisas da Amazônia, Coordenação de Uso da Terra e Mudança Climática, Manaus, AM - Brasil. E-mail: <rmarengo@inpa.gov.br>.

\*Corresponding author.

**ABSTRACT** – The simultaneous effect of elevated CO<sub>2</sub> concentration and drought on trees is still under investigation in the Amazon. We evaluated the effect of CO<sub>2</sub> levels (400 and 800 ppm) and water regimes (50% and 100% soil field capacity) on photosynthetic traits, chlorophyll fluorescence, and total biomass accumulation in *Ceiba pentandra*. In well-watered plants, light-saturated photosynthesis ( $P_{N-sat}$ ) increased in plants exposed to elevated CO<sub>2</sub>, but both  $P_{N-sat}$  and stomatal conductance decreased in response to water deficit. The maximum carboxylation rate of Rubisco declined under elevated CO<sub>2</sub>, which indicates down-regulation of photosynthesis at elevated CO<sub>2</sub>. The  $F_v/F_m$  ratio was not affected by treatments. Notwithstanding, total plant biomass and leaf area were reduced by 34-37% under water deficit, but they were not affected by CO<sub>2</sub> levels. The  $P_{N-sat}$  values measured in well-irrigated plants at ambient CO<sub>2</sub> were similar to those observed in plants subjected to elevated CO<sub>2</sub> and water deficit ( $p = 0.26$ ). We concluded that the effect of water deficit on  $P_{N-sat}$  was mitigated by elevated CO<sub>2</sub>. These results suggest that the increase of atmospheric CO<sub>2</sub> concentrations associated to climate changes can at least partly offset the negative effect of drought in this multiuse and widely distributed species.

Keywords: Biomass accumulation; Water use efficiency; Photosynthesis acclimation.

## O CO<sub>2</sub> ELEVADO INDUZ A REGULÇÃO NEGATIVA DA FOTOSÍNTESE E ALIVIA O EFEITO DO DÉFICIT HÍDRICO EM *Ceiba pentandra* (MALVACEAE)

**RESUMO** – O efeito simultâneo do aumento da concentração de CO<sub>2</sub> e da seca nas árvores ainda está sendo investigado na Amazônia. Avaliou-se o efeito de níveis de CO<sub>2</sub> (400 e 800 ppm) e regimes hídricos (50% e 100% da capacidade de campo do solo) sobre características fotossintéticas, fluorescência da clorofila e acúmulo de biomassa total em *Ceiba pentandra*. Em plantas bem irrigadas, a fotossíntese saturada por luz ( $P_{N-sat}$ ) aumentou em plantas expostas a CO<sub>2</sub> elevado, mas tanto  $P_{N-sat}$  quanto a condutância estomática diminuíram em resposta ao déficit hídrico. A taxa máxima de carboxilação de Rubisco diminuiu sob CO<sub>2</sub> elevado, o que indica regulação negativa da fotossíntese em CO<sub>2</sub> elevado. A relação  $F_v/F_m$  não foi afetada pelos tratamentos. No entanto, a biomassa total da planta e a área foliar foram reduzidas em 34-37% sob déficit hídrico, mas não foram afetadas pelos níveis de CO<sub>2</sub>. Os valores de  $P_{N-sat}$  medidos em plantas bem irrigadas em CO<sub>2</sub> ambiente foram semelhantes aos observados em plantas submetidas a CO<sub>2</sub> elevado e déficit hídrico ( $p = 0,26$ ). Assim, concluiu-se que o efeito do déficit hídrico no  $P_{N-sat}$  foi mitigado pelo CO<sub>2</sub> elevado. Estes resultados sugerem que o aumento das concentrações atmosféricas de CO<sub>2</sub> associado às mudanças climáticas pode compensar, pelo menos em parte, o efeito negativo da seca nesta espécie multiuso e amplamente distribuída.

Palavras-Chave: Acumulação de biomassa; Eficiência do uso da água; Acimação da fotossíntese.



## 1. INTRODUCTION

Climate models predict that temperature and atmospheric CO<sub>2</sub> concentration will continue to rise and at a global scale CO<sub>2</sub> concentrations can reach about 700 ppm by 2100. Because of the importance of the Amazon rainforest to global carbon and water cycle, efforts have been made to improve the understanding of potential effects of climatic variables on photosynthesis and growth of Amazonian trees (Marenco et al., 2014; Silveira et al., 2023).

Plant responses to elevated CO<sub>2</sub> have been studied for years, and it has been found that in the short-term (minutes to hours) photosynthesis almost always increases under elevated CO<sub>2</sub> (Delucia et al., 1985; Rogers and Ellsworth, 2002; Krämer et al., 2022). However, in the long-term (days to weeks) down-regulation of photosynthesis to elevated CO<sub>2</sub> can occur (Rogers and Humphries, 2000; Wang and Wang, 2021; Krämer et al., 2022). Down-regulation of photosynthesis has been attributed to acclimation of the photosynthetic apparatus to elevated CO<sub>2</sub> (e.g. reduction in the amount of Rubisco), and it has been defined as a decrease in maximum carboxylation rate of Rubisco (Rogers and Ellsworth, 2002; Kitao et al., 2007). Although much research has been done to assess the effect of elevated CO<sub>2</sub> on photosynthesis, the simultaneous effect of elevated CO<sub>2</sub> and water deficit is still under investigation in rainforest tropical trees. Indeed, the effect of elevated CO<sub>2</sub> on photosynthetic of trees has been evaluated only in a relatively small number of trees of the Amazon region (Oliveira and Marenco, 2019; Ferrer, 2021), which justifies carrying out further studies on this subject.

The exposure of plants to high [CO<sub>2</sub>] generally causes two physiological effects, a direct impact on photosynthesis and an indirect effect closely related to water economy. Subjecting a plant to high CO<sub>2</sub> concentration often leads to an increase in photosynthesis and plant biomass (Delucia et al., 1985; Curtis and Wang, 1998; Kitao et al., 2007; Way et al., 2015). The indirect effect of subjecting the plant to high CO<sub>2</sub> improves water use efficiency, as stomatal conductance may decrease at elevated CO<sub>2</sub> (Medlyn et al., 2001; Gao et al., 2015; Oliveira and Marenco, 2019; Ainsworth and Long, 2021). The increase in water use efficiency is important because associated with climatic variability the rainfall pattern

can change. For instance, it seems that droughts may become more frequent in Northeastern Brazil and part of the Amazon region (Cai et al., 2020).

Droughts cause a reduction in soil water content and an increase in vapor pressure deficit, which can lead to a decline in photosynthesis and tree growth, and eventually to an increase in mortality of trees under severe drought (Duffy et al., 2015; Marenco and Antezana-Vera, 2021; Camargo and Marenco, 2023). Plant response to water deficit varies with plant species, severity and duration of the drought stress (Kaur and Asthir, 2017; Fernando and Marenco, 2023). Parameters such as stomatal conductance, photosynthesis and leaf expansion are often modified even by mild water deficit, while reduced growth is a common response to prolonged droughts (Kaur and Asthir, 2017; Flexas et al., 2012; Oliveira and Marenco, 2019). Mild water deficit leads to a decline in photosynthesis due to partial stomatal closure, while under severe drought stomatal and non-stomatal limitation lead to a decline in carbon assimilation (Flexas et al., 2012; Wang and Wang, 2021). Moreover, under water deficit a reduction in photosynthesis occurs in parallel with an increase in the amount of energy not used in photochemical reactions, and hence non-photochemical quenching (energy dissipation as heat) is an essential mechanism to protect the leaf against high light stress (Ruban, 2016). Therefore, parameters of chlorophyll fluorescence have been commonly used to assess the performance of a leaf under water deficit (Rascher et al., 2004; Kitao et al., 2007; Yang et al., 2014). The aim of this study was to evaluate the effect of elevated CO<sub>2</sub> concentration and water deficit on biomass accumulation, photosynthesis and water use efficiency in *Ceiba pentandra*.

## 2. MATERIALS AND METHODS

### 2.1 Plant material and experimental conditions

The experiment was carried out at the Instituto Nacional de Pesquisas da Amazônia - INPA (03° 05'30" S, 59° 59'35" W), Manaus, between March and August of 2019. We used a greenhouse and a growth chamber with electronic control of CO<sub>2</sub> concentration and temperature. *Ceiba pentandra* (L.) Gaertn. (Malvaceae) grows relatively fast in the juvenile stage (Ribeiro et al., 2023). Under field conditions growth rates of 2.25 cm year<sup>-1</sup> in diameter and 24 cm year<sup>-1</sup> in

height have been reported (Keefe et al., 2009; Román-Dañobeytia et al., 2015). We selected *C. pentandra* not only because of its growth rates and large distribution throughout the Amazon Basin, Central and South America, but mainly due to its socio-economic potential, as besides producing timber and fibers, it also seems to have medicinal properties (Gómez-Maqueo and Gamboa-deBuen, 2022).

Seeds of *C. pentandra* were germinated in vermiculite and 15 days after emergence, the plants were transferred to pots (21 cm diameter and 17 cm deep), containing 4.5 kg of forest soil, which was fertilized with 5 g kg<sup>-1</sup>, as previously described (Silveira et al., 2023). After transplanting the plants were kept for 90 days in a greenhouse at ambient temperature (~27 °C) and ambient CO<sub>2</sub> concentration under well-watered conditions. Then, the plants (53 cm height and 7.0 mm stem diameter) were randomly assigned into four groups: two CO<sub>2</sub> levels (400 ppm and 800 ppm) and two water regimes within each CO<sub>2</sub> level. The water regimes were: soil at 50% and 100% field capacity, FC. Thus, the four treatments were: T<sub>1</sub>: 400/100, T<sub>2</sub>: 400/50, T<sub>3</sub>: 800/100, and T<sub>4</sub>: 800/50 (i.e. 800 ppm CO<sub>2</sub> and soil at 50% FC). The plants grew under these conditions for 138 days (hereafter referred to as the experimental period). The plants at ambient CO<sub>2</sub> (400 ppm) were grown in a greenhouse (four metal-frame sides (4 m tall) supporting an oval roof –6 m tall in the middle). The roof was covered with a double layer of 150-µm polyethylene film. In the greenhouse, mean photosynthetically active radiation (PAR) was 200 µmol m<sup>-2</sup> s<sup>-1</sup> (i.e. 8.6 mol m<sup>-2</sup> day<sup>-1</sup>), relative humidity was 70–80%, mean temperature of 27.5 °C (ranging from 26 °C at night to 29 °C at midday), and day/night ambient CO<sub>2</sub> concentration of 400/420 ppm). Thus, we used the daytime CO<sub>2</sub> concentration measured in the greenhouse to set the growth chamber at twice this value. The plants to be subjected to 800 ppm CO<sub>2</sub> were transferred to a growth chamber (TPC-1, Winnipeg, Canada). The growth chamber had a working area of 1.72 m<sup>2</sup>, 1.52 m internal height, with automatic control of temperature (HMP60 Vaisala, Vantaa, Finland) and CO<sub>2</sub> (GMM222, Vaisala).

## 2.2 Growth chamber conditions

Following the light conditions of the greenhouse, the PAR intensity in the growth chamber was set to a constant value of 200 µmol m<sup>-2</sup> s<sup>-1</sup> with a photoperiod

of 12 hours (6 am to 6 pm), while the CO<sub>2</sub> concentration was kept constant at 800 ppm (hereafter referred to as eCO<sub>2</sub>). The day/night temperature was set at 27/25 °C (average of 26 °C), and relative humidity was 80% (daytime) and 90% (nighttime). The irradiance used in this experiment was about 26% of total PAR in the open during 2019 (~33.0 mol m<sup>-2</sup> day<sup>-1</sup>, computed from INMET's data; INMET, 2023).

## 2.3 Soil water content and water regimes

Before subjecting the plants to the water regimes, we gravimetrically determined the amount of water (volume) the soil could hold at field capacity –FC (100% FC). Half of this value was added to the soil to be kept at 50% FC. During the experiment, every other day, the pots were weighed (7 am to 8 am) to measure the amount of water consumed by the plant, and then it was replaced to keep the soil water content at its target value (50% or 100% FC); in this calculation, the daily fresh weight gain of the plant was taken into account. Evaporation from the soil surface was prevented by covering the pot with a plastic bag and tying it off at the base of the stem. To estimate the daily contribution of fresh plant growth (PFW) to the pot total mass (i.e. pot, soil, water and fresh plant mass) an allometric equation was used (Silveira et al., 2023):

$$\text{PFW (g, FW)} = 3.838 \exp(0.2861 \times D) \quad \text{Eq.1}$$

where *D* is the stem diameter in millimeter.

The plants were subjected to eCO<sub>2</sub> and water deficit treatments for 138 days (March – August 2019), enough time for the plant to produce new leaves under the treatment conditions. At the end of the experimental period, we measured photosynthetic traits, fluorescence parameters, SPAD values (a measure of the relative chlorophyll content), leaf nitrogen, leaf total non-structural carbohydrates (TNC), and water potential in leaves produced during the experimental period.

## 2.4 Gas-exchange measurements

Photosynthetic traits were measured using a portable infrared gas analyzer (Li-6400XT, Li-Cor, Lincoln, NE, USA). Gas-exchange measurements were carried out between 8 am and 2 pm on two fully expanded leaves per plant from the upper third. At light saturation (1000 µmol m<sup>-2</sup> s<sup>-1</sup>) and [CO<sub>2</sub>] of treatments (400 ppm CO<sub>2</sub> for ambient conditions and 800 ppm

for elevated CO<sub>2</sub>) we measured light-saturated photosynthesis ( $P_{N-sat}$ ), stomatal conductance ( $g_{s-sat}$ ), transpiration ( $E_{sat}$ ), water use efficiency (WUE,  $P_{N-sat}/E_{sat}$ ), intrinsic WUE ( $WUE_i, P_{N-sat}/g_{s-sat}$ ), leaf to air vapor pressure difference ( $VPD_L$ ), and dark respiration ( $R_d$ , measured at a PAR value of zero, after a stabilization period of 3-5 min). While at light and CO<sub>2</sub> saturation (2000 ppm CO<sub>2</sub>) we measured photosynthesis ( $P_{N-max}$ ) and stomatal conductance ( $g_{s-max}$ ). Gas-exchange data were measured after a stabilization period of about 10 min at [CO<sub>2</sub>] of 400 ppm in the leaf chamber (about 240 ppm of internal CO<sub>2</sub> concentration –  $C_i$ ) and PAR of 250–500  $\mu\text{mol m}^{-2} \text{s}^{-1}$ . The PAR value at light saturation (1000  $\mu\text{mol m}^{-2} \text{s}^{-1}$ ) was determined after constructing a light-response curve (500, 250, 100, 75, 50, 25, 12, 0, 500 1000 and 2000  $\mu\text{mol m}^{-2} \text{s}^{-1}$ ). We also generated a  $P_N/C_i$  curve, by measuring  $P_N$  at light saturation and varying CO<sub>2</sub> concentration in the leaf chamber [400, 250 100, 0\*, 400, 1000, 1500 and 2000 ppm]. The 0\* corresponds to the [CO<sub>2</sub>] obtained by turning the mixer off. We used the  $P_N/C_i$  data for computing the maximum carboxylation rate of Rubisco ( $V_{cmax}$ , expressed at 25 °C) and the maximum electron transport rate ( $J_{max}$ , at 25 °C), after Farquhar et al. (1980).

## 2.5 Fluorescence parameters

Chlorophyll fluorescence was determined at environmental conditions (~ 400 ppm of CO<sub>2</sub> and 27 °C) with a modulated fluorometer (PAM-2500, Walz GmbH, Effeltrich, Germany). These measurements were made on the same leaves used to determine gas-exchange. Early in the morning on a dark-adapted leaf (30 min dark-adaptation), the minimum ( $F_0$ ) and maximum fluorescence ( $F_m$ ) were measured. The  $F_m$  was obtained by applying a light pulse (6,000  $\mu\text{mol m}^{-2} \text{s}^{-1}$  for 1.0 s) and the  $F_v/F_m$  ratio (maximal quantum yield of photosystem II) computed as described by Rascher et al. (2004):

$$F_v/F_m = (F_m - F_0)/F_m \quad \text{Eq.2}$$

At midday and under actinic light (230  $\mu\text{mol m}^{-2} \text{s}^{-1}$ ) we also measured the effective quantum yield of photosystem II,  $\Phi_{PSII}$  (Rascher et al., 2004):

$$\Phi_{PSII} = (F_m' - F_s)/F_m' \quad \text{Eq.3}$$

where  $F_s$  and  $F_m'$  denote the steady-state and maximal fluorescence of the light-adapted state, respectively. While the non-photochemical quenching (NPQ) was computed as (Rascher et al., 2004):

$$\text{NPQ} = (F_m - F_m')/F_m' \quad \text{Eq. 4}$$

## 2.6 Leaf nitrogen, SPAD, sugars, starch and water content

The amount of starch and sugars in a fresh leaf sample (~20 mg) were determined as described by Dubois et al. (1956). Then, total non-structural carbohydrate content was obtained by summing up the sugar and starch contents. Leaf nitrogen ( $N_L$ ) was determined by the classical Kjeldahl method (Miyazawa et al., 2009), while the SPAD value was measured (eight readings per leaf) with a chlorophyll meter (SPAD-502, Minolta, Osaka, Japan) in the same leaves used for measuring gas-exchange.

## 2.7 Plant biomass, leaf area, LAM and leaf water potential

At the end of the experimental period, the total plant dry mass was recorded after oven drying at 72 °C until constant mass. The leaf area was measured (Li-3000, Li-Cor, Lincoln, NE, USA), and then the leaf area per mass (LAM, sometimes called specific leaf area) obtained. Leaf water potential ( $\Psi_L$ ) was determined early in the morning (~6 am) and at midday (~12 noon) in one leaf per plant with a pressure chamber (1505 D, PMS Instrument Company, Albany, USA). In addition, the relative leaf water content (RWC) in two leaves per plant was also measured:

$$\text{RWC (\%)} = 100 \times \frac{\text{LFM} - \text{LDM}}{\text{LTM} - \text{LDM}} \quad \text{Eq.5}$$

where, LFM, LTM, and LDM represent the leaf fresh mass, leaf turgid mass and leaf dry mass, respectively, being the dry mass measured as previously described. The turgid mass was obtained after cutting the tip of the petiole under water, and then the leaf was covered with a plastic bag and placed in a dark room for 12 hours (overnight) for full hydration.

## 2.8 Experimental design and statistical analysis

The experimental design was a split-plot, with the CO<sub>2</sub> concentration (400 and 800 ppm) as the main plot and the water regime (50% and 100% FC) as the split-plot, with eight replications. Prior to statistical analyzes data were tested for normality (Shapiro–Wilks,  $\alpha = 0.05$ ), and log-transformed [ $\log(x+1)$ ] when necessary. Then the data were submitted to ANOVA and the means compared by the Fisher-LSD

test. We used  $p = 0.05$  to define statistical significance. Statistical analyzes were performed using Statistica version 7.0 (StatSoft, Inc. Tulsa OK, USA).

### 3. RESULTS

#### 3.1 Gas-exchange and chlorophyll fluorescence

Over water regimes, light-saturated photosynthesis ( $P_{N-sat}$ ) increased by 38% at eCO<sub>2</sub>

(mean of  $6.18 \mu\text{mol m}^{-2} \text{s}^{-1}$  at ambient CO<sub>2</sub> versus  $8.90 \mu\text{mol m}^{-2} \text{s}^{-1}$  at eCO<sub>2</sub>), and over CO<sub>2</sub> levels it decreased by 26% under water deficit (Fig. 1A). The effect of eCO<sub>2</sub> on  $g_{s-sat}$  was non-significant over water regimes ( $p = 0.246$ , Fig. 1B), but irrespective of the CO<sub>2</sub> level,  $g_{s-sat}$  decreased by 50% under water deficit. That is, under well-watered conditions  $g_{s-sat}$  was as high at ambient CO<sub>2</sub> as at eCO<sub>2</sub> ( $0.099$  and  $0.106 \text{ mol m}^{-2} \text{s}^{-1}$ , respectively; i.e., a  $g_{s-sat}$  ratio (eCO<sub>2</sub> to ambient

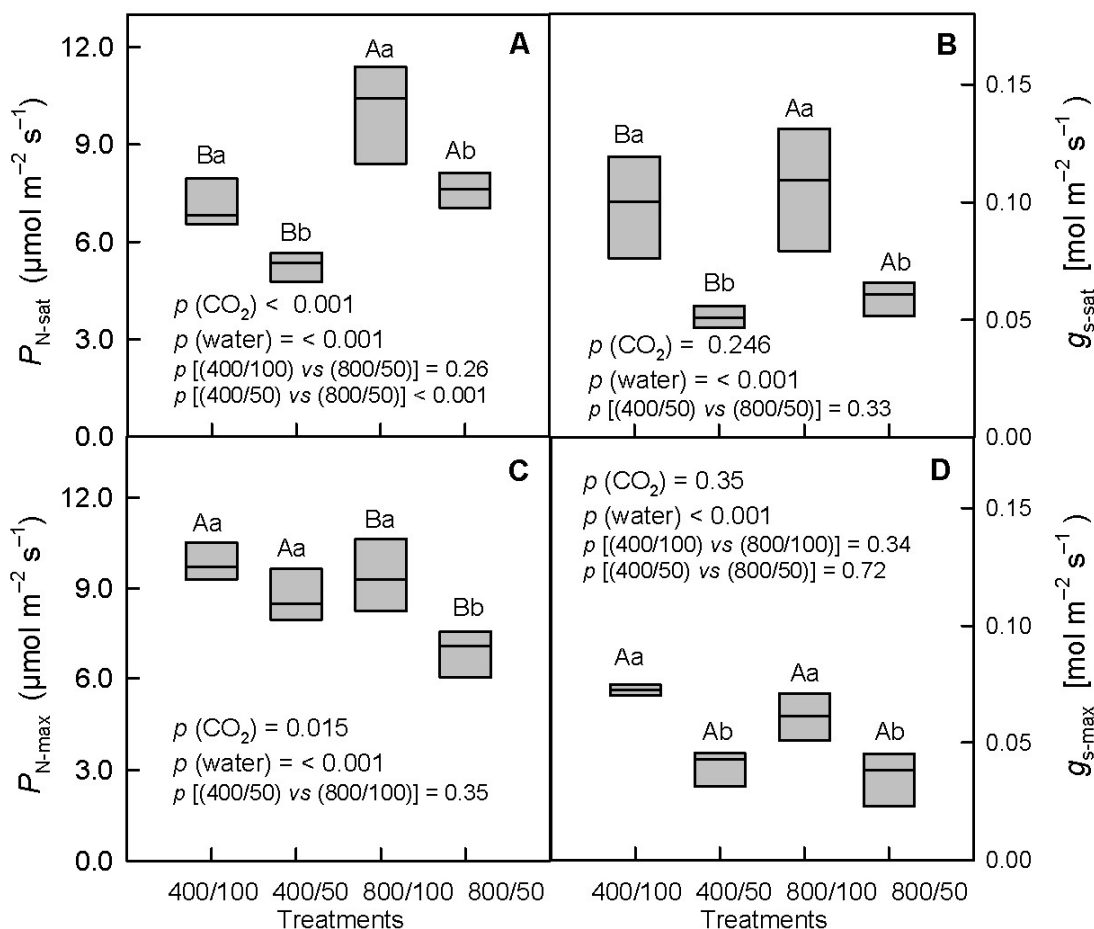


**Figure 1** – Light-saturated photosynthesis ( $P_{N-sat}$ , A) and stomatal conductance at light saturation ( $g_{s-sat}$ , B). Light and CO<sub>2</sub> saturated photosynthesis ( $P_{N-max}$ , C) and light and CO<sub>2</sub> saturated stomatal conductance ( $g_{s-max}$ , D) in *Ceiba pentandra* subjected to two CO<sub>2</sub> levels (400 and 800 ppm) and two water regimes –water (soil at 50% and 100% FC). In the boxes, different uppercase and different lowercase letters indicate differences between CO<sub>2</sub> levels (over water regimes) and water regimes (over CO<sub>2</sub> levels), respectively (Fisher LSD test,  $p = 0.05$ ,  $n = 8$ ). For clarity, the  $p$  values between some specific treatments are also shown.

**Figura 1** – Fotossíntese ( $P_{N-sat}$ , A) e condutância estomática em luz saturante ( $g_{s-sat}$ , B). Fotossíntese ( $P_{N-max}$ , C) e condutância estomática saturada de luz e CO<sub>2</sub> ( $g_{s-max}$ , D) em *Ceiba pentandra* submetida a dois níveis de CO<sub>2</sub> (400 e 800 ppm) e dois regimes hídricos –water (solo a 50% e 100% FC). Nas caixas, letras maiúsculas e minúsculas diferentes indicam diferenças entre níveis de CO<sub>2</sub> (nos regimes hídricos) e regimes hídricos (nos níveis de CO<sub>2</sub>), respectivamente (teste Fisher LSD,  $p = 0,05$ ,  $n = 8$ . Por clareza, os valores de  $p$  entre alguns tratamentos específicos são também mostrados.

**Table 1** – Leaf and plant traits of *Ceiba pentandra* subjected to two CO<sub>2</sub> levels (400 and 800 ppm) and two water regimes (soil at 100% and 50% FC). Different uppercase letters and different lowercase letters indicate differences between CO<sub>2</sub> levels and water regimes, respectively (Fisher LSD test,  $p = 0.05$ ,  $n = 8$ ). Means ( $\pm$  SD) of CO<sub>2</sub> levels and water regimes ( $n = 16$ ) are also shown.

Abbreviations:

$\Psi_L$ , leaf water potential;  $\Psi_{L-6h}$ ,  $\Psi_L$  measured at 6 am;  $\Psi_{L-12h}$ ,  $\Psi_L$  measured at 12 noon;  $R_d$ , leaf respiration; VPD<sub>L</sub>, leaf to air vapor pressure difference;  $E_{sat}$ , leaf transpiration at light saturation; WUE, water use efficiency; WUE<sub>i</sub>, intrinsic WUE;  $F_v/F_m$ , maximal quantum yield of PSII;  $\Phi_{PSII}$ , effective quantum yield of PSII; NPQ, non-photochemical quenching; LAM, leaf area per mass; RWC, relative water content; TNC, total non-structural carbohydrates;  $N_L$ , leaf nitrogen;  $W_d$ , total dry matter;  $A_L$ , total leaf area. SPAD values (a measure of the relative chlorophyll content); PSII, photosystem II; FC, Field capacity (of soil).

**Tabela 1** – Características da folha e da planta de *Ceiba pentandra* submetidas a dois níveis de CO<sub>2</sub> (400 e 800 ppm) e dois regimes hídricos (solo a 100% e 50% FC). Diferentes letras maiúsculas e diferentes letras minúsculas indicam diferenças entre os níveis de CO<sub>2</sub> e os regimes hídricos, respectivamente (teste Fisher LSD,  $p = 0,05$ ,  $n = 8$ ). As médias ( $\pm$  SD) dos níveis de CO<sub>2</sub> e regimes hídricos ( $n = 16$ ) são também mostradas.

Abreviações:

$\Psi_L$ , potencial hídrico foliar;  $\Psi_{L-6h}$ ,  $\Psi_L$  medido às 6h;  $\Psi_{L-12h}$ ,  $\Psi_L$  medido às 12, meio dia;  $R_d$ , respiração foliar; VPD<sub>L</sub>, diferença de pressão de vapor folha-ar;  $E_{sat}$ , transpiração foliar em luz saturante; WUE, eficiência no uso da água; WUE<sub>i</sub>, WUE intrínseca;  $F_v/F_m$ , rendimento quântico máximo do PSII;  $\Phi_{PSII}$ , rendimento quântico efetivo do PSII; NPQ, dissipação não fotoquímica; LAM, área foliar por massa; RWC, teor relativo de água; TNC, carboidratos não estruturais totais;  $W_d$ , matéria seca total;  $N_L$ , nitrogênio foliar;  $A_L$ , área foliar total. Valores SPAD (estimativa do teor relativo de clorofila); PSII, fotossistema II; FC, capacidade de campo (do solo).

Parameter	400 ppm		800 ppm		400 ppm	800 ppm	100% FC	50%FC
	100% FC	50% FC	100% FC	50% FC				
$\Psi_{L-6h}$ (MPa)	-0.28±0.02	-0.37±0.03	-0.35±0.04	-0.48±0.1	-0.32±0.05 <sup>A</sup>	-0.41±0.1 <sup>B</sup>	-0.31±0.05 <sup>a</sup>	-0.42±0.09 <sup>b</sup>
$\Psi_{L-12h}$ (MPa)	-0.69±0.1	-0.94±0.15	-0.61±0.07	-0.66±0.05	-0.82±0.18 <sup>B</sup>	-0.64±0.06 <sup>A</sup>	-0.65±0.09 <sup>a</sup>	-0.80±0.18 <sup>b</sup>
$R_d$ ( $\mu\text{mol m}^{-2} \text{s}^{-1}$ )	0.41±0.04	0.38±0.04	0.43±0.13	0.41±0.11	0.40±0.04 <sup>A</sup>	0.42±0.12 <sup>A</sup>	0.42±0.09 <sup>a</sup>	0.40±0.08 <sup>a</sup>
VPD <sub>L</sub> (kPa)	1.31±0.10	1.54±0.09	1.31±0.14	1.44±0.10	1.42±0.15 <sup>A</sup>	1.38±0.14 <sup>A</sup>	1.31±0.12 <sup>b</sup>	1.49±0.10 <sup>a</sup>
$E_{sat}$ ( $\text{mmol m}^{-2} \text{s}^{-1}$ )	1.21±0.26	0.77±0.06	1.28±0.36	0.83±0.14	0.99±0.29 <sup>A</sup>	1.06±0.35 <sup>A</sup>	1.24±0.30 <sup>a</sup>	0.80±0.11 <sup>b</sup>
WUE ( $\text{mmol mol}^{-1}$ )	6.2±0.6	6.9±0.4	8.6±2.0	9.7±2.3	6.50±0.6 <sup>B</sup>	9.10±2.2 <sup>A</sup>	7.4±1.9 <sup>a</sup>	8.3±2.2 <sup>a</sup>
WUEi ( $\mu\text{mol mol}^{-1}$ )	77.5±15.1	104.7±3.0	110.0±35.2	139.7±34.7	91.1±17.5 <sup>B</sup>	124.8±37.1 <sup>A</sup>	93.7±31.1 <sup>b</sup>	122.2±29.9 <sup>a</sup>
$F_v/F_m$	0.75±0.02	0.74±0.01	0.74±0.04	0.72±0.03	0.74±0.02 <sup>A</sup>	0.73±0.03 <sup>A</sup>	0.74±0.03 <sup>a</sup>	0.73±0.02 <sup>a</sup>
$\Phi_{PSII}$	0.54±0.04	0.44±0.07	0.53±0.04	0.47±0.06	0.49±0.07 <sup>A</sup>	0.50±0.06 <sup>A</sup>	0.53±0.04 <sup>a</sup>	0.46±0.07 <sup>b</sup>
NPQ	5.41±0.21	6.84±0.32	4.95±0.24	5.27±0.29	6.13±0.26 <sup>A</sup>	5.11±0.19 <sup>B</sup>	5.18±0.17 <sup>b</sup>	6.05±0.29 <sup>a</sup>
LAM ( $\text{m}^2 \text{kg}^{-1}$ )	24.4±1.1	24.4±1.8	20.8±1.8	20.4±1.3	24.4±1.4 <sup>A</sup>	20.6±1.5 <sup>B</sup>	22.6±2.3 <sup>a</sup>	22.4±2.6 <sup>a</sup>
RWC (%)	88.2±2.6	87.5±2.1	89.2±5.2	82.7±3.6	87.8±2.3 <sup>A</sup>	86.0±5.5 <sup>A</sup>	88.7±4.0 <sup>a</sup>	85.1±3.8 <sup>b</sup>
Sugar ( $\text{g m}^{-2}$ )	1.94±0.19	1.58±0.18	2.02±0.42	2.30±0.15	1.76±0.26 <sup>B</sup>	2.16±0.34 <sup>A</sup>	1.98±0.31 <sup>a</sup>	1.94±0.41 <sup>a</sup>
Starch ( $\text{g m}^{-2}$ )	6.41±0.38	6.28±0.91	8.53±1.16	8.69±0.81	6.34±0.68 <sup>B</sup>	8.61±0.97 <sup>A</sup>	7.47±1.38 <sup>a</sup>	7.49±1.50 <sup>a</sup>
TNC ( $\text{g m}^{-2}$ )	8.3±0.4	7.9±0.9	10.6±1.5	11.0±0.9	8.1±0.7 <sup>B</sup>	10.8±1.2 <sup>A</sup>	9.5±1.5 <sup>a</sup>	9.4±1.8 <sup>a</sup>
$N_L$ ( $\text{g m}^{-2}$ )	1.07±0.06	1.10±0.12	1.16±0.17	1.15±0.08	1.09±0.10 <sup>A</sup>	1.15±0.13 <sup>A</sup>	1.12±0.14 <sup>a</sup>	1.13±0.10 <sup>a</sup>
$W_d$ (g per plant)	33.3±3.7	19.3±2.2	29.4±4.2	21.7±5.1	26.3±7.8 <sup>A</sup>	25.5±6.0 <sup>A</sup>	31.3±4.3 <sup>a</sup>	20.5±4.0 <sup>b</sup>
$A_L$ ( $\text{m}^2$ per plant)	0.25±0.05	0.17±0.03	0.24±0.02	0.14±0.04	0.21±0.06 <sup>A</sup>	0.19±0.06 <sup>A</sup>	0.24±0.04 <sup>a</sup>	0.15±0.04 <sup>b</sup>
SPAD values	51.6±2.8	50.9±1.7	49.8±5.9	36.7±6.4	51.3±2.3 <sup>A</sup>	43.3±9.0 <sup>B</sup>	50.7±4.6 <sup>a</sup>	43.8±8.6 <sup>b</sup>

CO<sub>2</sub>) of 1.07). Leaf transpiration ( $E_{sat}$ ) decreased under water deficit, following an increase in VPD<sub>L</sub> under limited water supply (Table 1).

Despite the decline of stomatal conductance ( $g_{s-sat}$ ) in plants subjected to water deficit, the  $P_{N-sat}$  values measured in well-irrigated plants grown at ambient CO<sub>2</sub> were similar to those found in plants subjected to elevated CO<sub>2</sub> and water deficit (7.12 and 7.64  $\mu\text{mol m}^{-2} \text{s}^{-1}$ ,  $p = 0.26$ ), being the lowest  $P_{N-sat}$  values observed in plants grown at ambient CO<sub>2</sub> and subjected to water deficit (Fig. 1A).

Under light and CO<sub>2</sub> saturation, photosynthetic rates ( $P_{N-max}$ ) were greatly reduced in plants subjected water deficit, which ultimately led to a significant

effect of eCO<sub>2</sub> and water deficit ( $p \leq 0.015$ , Fig. 1C). It should be noted, however, that there was no difference between the  $P_{N-max}$  values recorded in well irrigated plants and those recorded at ambient CO<sub>2</sub>, irrespective of water regime; for instance, there was no difference between plants grown at ambient CO<sub>2</sub> and limited water supply and those well-watered and exposed to eCO<sub>2</sub> ( $p = 0.35$ , Fig. 1C). The stomatal conductance measured at CO<sub>2</sub> saturation ( $g_{s-max}$ ) was neutral to the effect of eCO<sub>2</sub> ( $p = 0.35$ ), but it decreased under water deficit ( $p < 0.001$ , Fig. 1D). Regarding the loss of carbon by respiration, both eCO<sub>2</sub> and water deficit had no significant effect on leaf respiration (Table 1).

Over water regimes, the  $V_{cmax}$  values were lower in plants exposed to eCO<sub>2</sub> than in those grown at

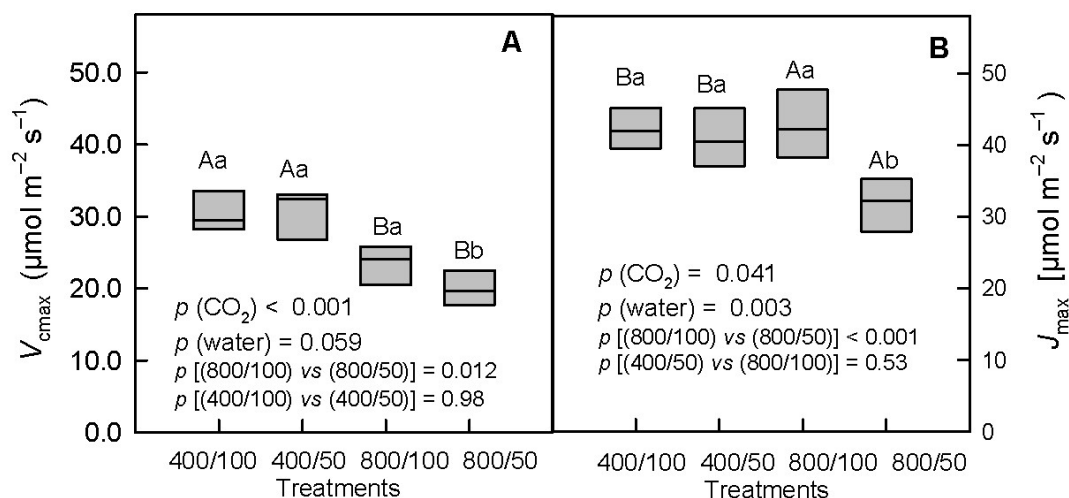


**Figure 2** – Maximum carboxylation rate of Rubisco ( $V_{cmax}$ , A) and maximum electron transport rate ( $J_{max}$ , B) in *Ceiba pentandra* subjected to two CO<sub>2</sub> levels (400 and 800 ppm) and two water regimes –water (soil at 50% and 100% FC). Further information as shown in Fig. 1.

**Figura 2** – Taxa máxima de carboxilação da Rubisco ( $V_{cmax}$ , A) e taxa máxima de transporte de elétrons ( $J_{max}$ , B) em *Ceiba pentandra* submetida a dois níveis de CO<sub>2</sub> (400 e 800 ppm) e dois regimes de hídricos – water (solo a 50% e 100% FC). Mais informações conforme mostrado na Fig. 1.

ambient CO<sub>2</sub> (22.3 versus 30.6  $\mu\text{mol m}^{-2} \text{s}^{-1}$ ,  $p < 0.01$ , Fig. 2A). Because the  $V_{cmax}$  values recorded at ambient CO<sub>2</sub> were very close ( $\sim 30.5 \mu\text{mol m}^{-2} \text{s}^{-1}$ ,  $p = 0.98$ ), on average the effect of water stress over CO<sub>2</sub> levels did not reach the level of significance ( $p = 0.059$ , Fig. 2A). However, it is worth noting, that  $V_{cmax}$  significantly diminished at eCO<sub>2</sub> under water deficit ( $p = 0.012$ , Fig. 2A). The  $J_{max}$  –likewise  $P_{N-max}$  – only decreased in plants subjected to eCO<sub>2</sub> and water deficit ( $p < 0.001$ ), and as a result, the effects of both eCO<sub>2</sub> and water deficit on  $J_{max}$  were significant (Fig. 2B). Thus, it can be noted, that there was no difference between  $J_{max}$  recorded at ambient CO<sub>2</sub> and the  $J_{max}$  measured at eCO<sub>2</sub> in well-irrigated plants (Fig. 2B).

On average, water use efficiency (WUE) was 40% higher in plants subjected to eCO<sub>2</sub> than in those grown at ambient CO<sub>2</sub> (9.10  $\text{mmol mol}^{-1}$  versus 6.50  $\text{mmol mol}^{-1}$ ). Although WUE tended to increase by 12% under water limitation, the effect of water deficit on WUE was not significant (Table 1). On average, WUE<sub>i</sub> ( $P_{N-sat}/g_{s-sat}$ ) was responsive to both eCO<sub>2</sub> and water regimes (Table 1), while the leaf water potential ( $\Psi_l$ ) was lower under water deficits than in well-irrigated plants, and lower at midday than early in the morning (Table 1). Likewise, the relative water

content (RWC) of leaves varied from 85.1% in plants under water deficit to 88.7% in well-irrigated plants ( $p \leq 0.05$ , Table 1).

Regarding the effect of treatments on leaf photochemistry, both eCO<sub>2</sub> and water deficit had a neutral effect on the  $F_v/F_m$  ratio (Table 1). On the other hand, the  $\Phi_{PSII}$  decreased under water deficit (0.46 versus 0.53,  $p \leq 0.05$ , Table 1), but the effect of eCO<sub>2</sub> was not significant ( $p > 0.05$ ). Whereas, NPQ decreased at eCO<sub>2</sub> and rose under water deficit, particularly in plants grown at ambient CO<sub>2</sub> conditions ( $p \leq 0.05$ , Table 1).

### 3.2 Nitrogen, TNC, and biomass accumulation

Sugar and starch content increased at eCO<sub>2</sub>, and hence the total non-structural carbohydrates (TNC) content also augmented (8.1  $\text{g m}^{-2}$  at ambient CO<sub>2</sub> against 10.8  $\text{g m}^{-2}$  at eCO<sub>2</sub>, Table 1). Water deficit, however, had no effect on sugar or starch content. Likewise, the leaf area per mass (LAM) was only affected by eCO<sub>2</sub>. While, neither eCO<sub>2</sub> nor water deficit had a significant effect on leaf nitrogen (Table 1). The total plant dry matter ( $W_T$ ) was reduced 34.5% under water deficit (31.3 versus 20.5  $\text{g per plant}$ ), and similarly the total leaf area per plant declined 37.5%

under limited water supply, but the effect of eCO<sub>2</sub> on  $W_T$  and total leaf area was not significant (Table 1).

#### 4. DISCUSSION

We found that  $P_{N-sat}$  increased at eCO<sub>2</sub> in well irrigated plants, but irrespective of the CO<sub>2</sub> level, it decreased under water deficit. Moreover, the  $P_{N-sat}$  values were as high in well-watered plants at ambient CO<sub>2</sub> as in those at eCO<sub>2</sub> under water stress. Stomatal conductance ( $g_{s-sat}$ ) was unresponsive to eCO<sub>2</sub>, but it dropped under water deficit. The  $V_{cmax}$  values decreased at eCO<sub>2</sub>, but the effect of water deficit was only significant at eCO<sub>2</sub>, while the  $F_v/F_m$  ratio and the effective quantum yield ( $\Phi_{PSII}$ ) were unaffected by the CO<sub>2</sub> treatments. Both plant dry matter and leaf area were unresponsive to eCO<sub>2</sub>, but plant biomass and leaf area diminished under water deficit.

The increase in photosynthesis ( $P_{N-sat}$ ) at eCO<sub>2</sub> is consistent with classic response of an increase in photosynthetic rates in response to exposure to eCO<sub>2</sub> (Rogers and Humphries, 2000; Gao et al., 2015; Oliveira and Marengo, 2019; Ainsworth and Long, 2021). Furthermore, subjecting the plants to eCO<sub>2</sub> mitigated the negative effect water deficit on photosynthesis, as  $P_{N-sat}$  values of well-irrigated plants at ambient CO<sub>2</sub> were comparable with those measured at eCO<sub>2</sub> under water deficit, even when stomatal conductance dropped under limited water supply (Fig 1A), which is consistent with the results reported by Oliveira and Marengo (2019) and Wang and Wang (2021). This is important and suggests that the steady increase of atmospheric CO<sub>2</sub> concentrations may at least partially alleviate the negative effect of drought on carbon assimilation.

Stomatal conductance ( $g_{s-sat}$ ) did not decrease at eCO<sub>2</sub> under well-watered conditions, which is contrary to what has been reported by others (Kitao et al., 2007; Wang and Wang, 2021; Ainsworth and Long, 2021). However, it has also been found that eCO<sub>2</sub> may have a neutral effect on stomatal conductance (Curtis and Wang, 1998). Not to mention that Santrucek and Sage (1996) reported that eCO<sub>2</sub> may attenuate the response of stomatal conductance ( $g_s$ ) to CO<sub>2</sub>. The eCO<sub>2</sub> to ambient CO<sub>2</sub>  $g_s$  ratio reported in this study (1.07) is consistent with results reported by Medlyn et al. (2001) for experiments with eCO<sub>2</sub> exposure time of less than

one year, as they reported a  $g_s$  ratio (eCO<sub>2</sub>/ambient CO<sub>2</sub>) of 0.95 (95% confidence interval of 0.83-1.09). The decline of  $g_{s-sat}$  under water deficit concurs with the classic response of a drop in stomatal conductance due to water limitation (Kaur and Asthir, 2017; Oliveira and Marengo, 2019; Fernando and Marengo, 2023). The reduction of  $P_{N-max}$  at eCO<sub>2</sub> under water deficit (Fig. 1C) may reflect both a drop in stomatal conductance and a decrease in  $V_{cmax}$ . Thus, the decline in  $P_{N-max}$  may indicate the negative effect of stomatal and non-stomatal limitation. This is because a decrease in mesophyll conductance reduces carboxylation efficiency. Perez-Martin et al. (2014) reported that in *Olea europaea* the decrease in photosynthesis under severe drought was related to a drop in mesophyll conductance, while Flexas et al. (2012) reported that Rubisco activity can be negatively affected by water deficit, which can explain the decline in  $V_{cmax}$  under limited water supply and eCO<sub>2</sub>. Altogether, the decline of  $J_{max}$  and  $V_{cmax}$  at eCO<sub>2</sub> under water deficit indicates that non-stomatal factors can affect photosynthetic rates, as mesophyll conductance may decrease with increasing intercellular CO<sub>2</sub> concentration (Kitao et al., 2015). Although  $P_{N-sat}$  increased at eCO<sub>2</sub> (under well-watered conditions), there was a decline in  $V_{cmax}$  at eCO<sub>2</sub> ( $p < 0.001$ ), which led us to concluded that the exposure to high CO<sub>2</sub> concentration caused down-regulation of photosynthesis –the decline in  $V_{cmax}$  (Rogers and Humphries, 2000; Rogers and Ellsworth, 2002; Kitao et al., 2007). Although, a down-regulation of photosynthesis is not an uncommon response to eCO<sub>2</sub> (Rogers and Humphries, 2000; Wang and Wang, 2021; Krämer et al., 2022), no acclimation of photosynthesis to eCO<sub>2</sub> has also been reported (Curtis and Wang, 1998).

Water use efficiency (WUE) was improved at eCO<sub>2</sub>, which can be explained by the positive effect of eCO<sub>2</sub> on  $P_{N-sat}$  (Way et al., 2015; Gao et al., 2015). WUE also tended to increase under water deficit, but the effect of water scarcity did not reach the significance level ( $p > 0.05$ ). This occurred because the relative decline of  $P_{N-sat}$  under water deficit (25%, Fig. 1A) was lower than the drop in leaf transpiration (35%, Table 1). The increase in WUE<sub>i</sub> ( $P_{N-sat}/g_{s-sat}$ ) under water deficit occurred because the relative drop in stomatal conductance was larger than the relative decrease in photosynthetic rates, which was also reported by Oliveira and Marengo (2019) and Wang and Wang (2021). An increase in WUE<sub>i</sub> under eCO<sub>2</sub>

may contribute to improve plant tolerance to water deficit. This is important because climate changes can lead to prolonged droughts in parts of the Amazon region (Cai et al., 2020).

The lack of an effect of treatments on the  $F_v/F_m$  ratio indicates that both eCO<sub>2</sub> and water deficit did not alter leaf photochemistry, which was also observed in other species subjected to water deficit, and indicates absence of pre-dawn photoinhibition (Rascher et al., 2004; Kitao et al., 2007; Oliveira and Marengo, 2019). A decline in  $\Phi_{PSII}$  under water deficit (and hence an increase in NPQ) can be associated with a reduction in stomatal conductance and photosynthesis, as there is a direct relationship between stomatal conductance and  $\Phi_{PSII}$  (Jiang et al., 2006; Ahanger et al., 2020; Vanitha et al., 2022). In addition, water deficit can eventually affect the stability of membranes in chloroplasts. In rice, severe water deficit leads to an increase in superoxide radicals and membrane peroxidation, which can cause a reduction in  $\Phi_{PSII}$  and  $F_v/F_m$  values (Yang et al., 2014). However, in this experiment, it seems unlikely that membranes were damaged, as there was no change in the  $F_v/F_m$  ratio. Instead, the decline in  $\Phi_{PSII}$  under water deficit can be attributed to a decline in stomatal conductance, as mentioned above. Compared with well-watered plants, the increase of NPQ under water deficit shows that a larger amount of energy can be dissipated as heat when less energy is used in photochemical reactions (Ruban, 2016).

Starch has been reported to increase under CO<sub>2</sub>-enriched atmosphere (Kitao et al., 2007; Wang and Wang, 2021). The high TNC found at eCO<sub>2</sub> may have contributed to decrease LAM (i.e. to increase leaf mass per area). We found only a slight decrease in RWC, which is consistent with the small decline in leaf water potential ( $\Psi_L$ ) under water deficit. Taking well-irrigated plants as the baseline, at noon  $\Psi_L$  declined only 23% under water deficit (Table 1). This is in line with the results of Rascher et al. (2004), who observed that *C. pentandra* maintains relatively high leaf water potential during drought. A slight decline in  $\Psi_L$  in plants subjected to water deficit (Table 1) may indicate that *C. pentandra* has a tight control of leaf transpiration by reducing stomatal conductance under water deficit.

Even though  $P_{N-sat}$  increased at eCO<sub>2</sub> ( $p < 0.001$ ), we found no effect of eCO<sub>2</sub> on  $W_T$  (total plant biomass).

This can occur because plant growth is a complex process that reflects the balance between carbon gain by photosynthesis and total carbon loss, not only via plant respiration, but also due loss of carbon by root exudation, which can be higher under elevated CO<sub>2</sub> (Phillips et al., 2011). Also a high sensitivity of *C. pentandra* to ethylene may also contribute to the absence of a positive effect of eCO<sub>2</sub> on  $W_T$ . This is because, it has been reported that an increase in CO<sub>2</sub> concentration may promote ethylene biosynthesis (Seneweera et al., 2003), and high ethylene concentrations may reduce growth (Dai et al., 2023).

## 5. CONCLUSIONS

We found that light-saturated photosynthesis increased at elevated CO<sub>2</sub>, but it decreased under water deficit. Notwithstanding, plant biomass was neutral to the effect of elevated CO<sub>2</sub>. The elevated CO<sub>2</sub> improves water use efficiency and alleviates the effect of water limitation. We reach this conclusion because well-irrigated plants at ambient CO<sub>2</sub> and plants under elevated CO<sub>2</sub> and water deficit had similar  $P_{N-sat}$  values. The  $V_{cmax}$  decreased at elevated CO<sub>2</sub>, which suggests acclimatization of photosynthesis to elevated CO<sub>2</sub>. These results improve our understanding of the concomitant effect of elevated CO<sub>2</sub> and water deficit on the ecophysiology of *Ceiba pentandra*, an important multipurpose tree.

## AUTHOR CONTRIBUTIONS

Author contributions: AMFS: data curation, formal analysis, investigation, writing – original draft; RAM: conceptualization, formal analysis, funding acquisition, investigation, methodology, project administration, supervision, writing – review and editing.

## 6. ACKNOWLEDGMENTS

We thank the Ministério da Ciência, Tecnologia e Inovações (MCTI-INPA, PRJ15.120), Conselho Nacional de Desenvolvimento Científico e Tecnológico (CNPq), Fundação de Amparo à Pesquisa do Estado do Amazonas (Fapeam), and Coordenação de Aperfeiçoamento de Pessoal de Nível Superior (Capes). Financial support: Fapeam (projeto Posgrad/Fapeam 2022 and scholarship to AMFS), CNPq (fellowship to RAM, grant: 303913/2021–5) and Capes (Code 001).



## 7. REFERENCES

- Ahanger MA, Mir RA, Alyemeni MN, Ahmad P. Combined effects of brassinosteroid and kinetin mitigates salinity stress in tomato through the modulation of antioxidant and osmolyte metabolism. *Plant Physiology and Biochemistry*. 2020; 147: 31-42. <https://doi.org/10.1016/j.plaphy.2019.12.007>
- Ainsworth EA, Long SP. 30 years of free-air carbon dioxide enrichment (FACE): What have we learned about future crop productivity and its potential for adaptation? *Global Change Biology*. 2021; 27: 27-49. <https://doi.org/10.1111/gcb.15375>
- Cai W, Mcphaden MJ, Grimm AM, Rodrigues RR, Taschetto AS, Garreaud RD, et al. Climate impacts of the El Niño–southern oscillation on South America. *Nature Reviews Earth Environment*. 2020; 1: 215-231. <https://doi.org/10.1038/s43017-020-0040-3>
- Camargo MAB, Marengo RA. Stem growth of Amazonian species is driven by intra-annual variability in rainfall, vapor pressure and evapotranspiration. *Acta Botanica Brasílica*. 2023; 37: e20220219. <https://doi.org/10.1590/1677-941X-ABB-2022-0219>
- Curtis P, Wang X. A meta-analysis of elevated CO<sub>2</sub> effects on woody plant mass, form, and physiology. *Oecologia*. 1998; 113: 299–313. <https://doi.org/10.1007/s004420050381>
- Dai Z-H, Guan D-X, Bundschuh J, Ma LQ. Roles of phytohormones in mitigating abiotic stress in plants induced by metal (loid) s As, Cd, Cr, Hg, and Pb. *Critical Reviews in Environmental Science and Technology*. 2023; 53: 1310-1330. <https://doi.org/10.1080/10643389.2022.2134694>
- Delucia EH, Sasek TW, Strain BR. Photosynthetic inhibition after long-term exposure to elevated levels of atmospheric carbon dioxide. *Photosynthesis Research*. 1985; 7: 175–184. <https://doi.org/10.1007/BF00037008>
- Dubois M, Gilles KA, Hamilton JK, et al. Colorimetric method for determination of sugars and related substances. *Analytical Chemistry*. 1956; 28: 350-356. <https://doi.org/10.1021/ac60111a0177>
- Duffy PB, Brando P, Asner GP, Field CB. Projections of future meteorological drought and wet periods in the Amazon. *Proceedings of the National Academy of Sciences USA*. 2015; 112: 13172-13177. <https://doi.org/10.1073/pnas.1421010112>
- Farquhar GD, Von Caemmerer S, Berry JA. A biochemical model of photosynthetic CO<sub>2</sub> assimilation in leaves of C<sub>3</sub> species. *Planta*. 1980; 149: 78-90. <https://doi.org/10.1007/BF0038623>
- Fernando AM, Marengo RA. Successive soil drying and wetting cycles improve drought tolerance of Mangabeira. *Pesquisa Agropecuária Brasileira*. 2023; 58: (in press).
- Ferrer VR. Aumento da concentração de CO<sub>2</sub> e adição de fósforo nos fluxos de carbono e energia do processo fotossintético de plântulas de *Inga edulis* Mart. no sub-bosque da Amazônia Central [MS Dissertation]. Manaus, AM: Programa de Pós-Graduação em Ecologia. Instituto Nacional de Pesquisas da Amazônia; 2021. <https://repositorio.inpa.gov.br/handle/1/37916>
- Flexas J, Galle A, Galmes J, et al. The response of photosynthesis to soil water stress. In: Aroca R. (ed.): *Plant Responses to Drought Stress*, Springer-Verlag, Heidelberg; 2012. p. 129-144. [https://doi.org/10.1007/978-3-642-32653-0\\_3](https://doi.org/10.1007/978-3-642-32653-0_3)
- Gao, J, Han, X, Seneweera S, et al. Leaf photosynthesis and yield components of mung bean under fully open-air elevated [CO<sub>2</sub>]. *Journal Integrative Agriculture*. 2015; 14: 977-983. [https://doi.org/10.1016/S2095-3119\(14\)60941-2](https://doi.org/10.1016/S2095-3119(14)60941-2)
- Gómez-Maqueo X, Gamboa-deBuen A. The biology of the genus *Ceiba*, a potential source for sustainable production of natural fiber. *Plants*. 2022; 11: 521. <https://doi.org/10.3390/plants11040521>
- INMET - Instituto Nacional de Meteorologia. Gráficos climatológicos. 2023. [cited 2023 July 21]. Available at: <https://clima.inmet.gov.br/GraficosClimatologicos/AM/82331>.
- Jiang Q, Roche D, Monaco TA, Hole D. Stomatal conductance is a key parameter to assess limitations to photosynthesis and growth potential in barley genotypes. *Plant Biology*. 2006; 8: 515-521. <https://doi.org/10.1055/s-2006-923964>
- Kaur G, Asthir B. Molecular responses to drought stress in plants. *Biologia Plantarum*. 2017; 61: 201-

209. <https://doi.org/10.1007/s10535-016-0700-9>

Keefe K, Schulze MD, Pinheiro C, et al. Enrichment planting as a silvicultural option in the eastern Amazon: case study of Fazenda Cauaxi. *Forest Ecology Management*. 2009; 258: 1950-1959. <https://doi.org/10.1016/j.foreco.2009.07.037>

Kitao M, Lei TT, Koike T, et al. Interaction of drought and elevated CO<sub>2</sub> concentration on photosynthetic down-regulation and susceptibility to photoinhibition in Japanese white birch seedlings grown with limited N availability. *Tree Physiology*. 2007; 27: 727-735. <https://doi.org/10.1093/treephys/27.5.727>

Kitao M, Yazaki K, Kitaoka S, et al. Mesophyll conductance in leaves of Japanese white birch (*Betula platyphylla* var. *japonica*) seedlings grown under elevated CO<sub>2</sub> concentration and low N availability. *Physiologia Plantarum*. 2015; 155: 435-445. <https://doi.org/10.1111/ppl.12335>

Krämer K, Kepp G, Brock J, et al. Acclimation to elevated CO<sub>2</sub> affects the C/N balance by reducing de novo N assimilation. *Physiologia Plantarum*. 2022; 10: e13615. <https://doi.org/10.1111/ppl.13615>

Marenco RA, Antezana-Vera SA. Principal component regression analysis demonstrates the collinearity-free effect of sub estimated climatic variables on tree growth in the central Amazon. *Revista de Biologia Tropical*. 2021; 69: 482-493. <http://dx.doi.org/10.15517/rbt.v69i2.44489>

Marenco RA, Nascimento HCS, Magalhães, NS. Stomatal conductance in Amazonian tree saplings in response to variations in the physical environment. *Photosynthetica*. 2014; 52: 493-500. <https://doi.org/10.1007/s11099-014-0056-3>

Medlyn BE, Barton CVM, Broadmeadow MSJ, Ceulemans R, Angelis P, Forstreuter M. et al. 2001. Stomatal conductance of forest species after long-term exposure to elevated CO<sub>2</sub> concentration: a synthesis. *New Phytologist*. 2001; 149: 247-264. <https://doi.org/10.1046/j.1469-8137.2001.00028.x>

Miyazawa M, Pavan MA, Santana CAF, Melo WJ (2009) Análise química do tecido vegetal. In: Silva FC (eds) Manual de análises químicas de solos, plantas e fertilizantes. Brasília: Embrapa, pp 192-233.

Oliveira MF, Marenco RA. Photosynthesis and biomass accumulation in *Carapa surinamensis* (Meliaceae) in response to water stress at ambient and elevated CO<sub>2</sub>. *Photosynthetica*. 2019; 57: 137-146. <https://doi.org/10.32615/ps.2019.023>

Perez-Martin A, Michelazzo C, Torres-Ruiz JM, et al. Regulation of photosynthesis and stomatal and mesophyll conductance under water stress and recovery in olive trees: correlation with gene expression of carbonic anhydrase and aquaporins. *Journal of Experimental Botany*. 2014; 65: 3143-3156. <https://doi.org/10.1093/jxb/eru160>

Phillips RP, Finzi AC, Bernhardt ES. Enhanced root exudation induces microbial feedbacks to N cycling in a pine forest under long-term CO<sub>2</sub> fumigation. *Ecology Letters*. 2011; 14: 187-194. <https://doi.org/10.1111/j.1461-0248.2010.01570.x>

Rascher U, Bobich EG, Lin GH, et al. Functional diversity of photosynthesis during drought in a model tropical rainforest—the contributions of leaf area, photosynthetic electron transport and stomatal conductance to reduction in net ecosystem carbon exchange. *Plant Cell Environment*. 2004; 27: 1239-1256. <https://doi.org/10.1111/j.1365-3040.2004.01231.x>

Ribeiro VC, Martins-Souza M, Antezana-Vera SA, Marenco, RA. Does *Ceiba pentandra* (Malvaceae) a light demanding species succumb under deep shading? *Scientia Forestalis*. 2023; 51: e4005. <https://doi.org/10.18671/scifor.v51.25>

Rogers A, Ellsworth DS. Photosynthetic acclimation of *Pinus taeda* (loblolly pine) to long-term growth in elevated pCO<sub>2</sub> (FACE). *Plant, Cell and Environment*. 2002; 25: 851-858. <https://doi.org/10.1046/j.1365-3040.2002.00868.x>

Rogers A, Humphries SW. A mechanistic evaluation of photosynthetic acclimation at elevated CO<sub>2</sub>. *Global Change Biology*. 2000; 6: 1005-1011. <https://doi.org/10.1046/j.1365-2486.2000.00375.x>

Román-Dañobeytia F, Huayllani M, Michi A, Ibarra F, Loayza-Muro R, Vázquez T, et al. Reforestation with four native tree species after abandoned gold mining in the Peruvian Amazon. *Ecological Engineering*. 2015; 85: 39-46. <http://dx.doi.org/10.1016/j.ecoleng.2015.09.075>

Ruban AV. Non photochemical chlorophyll fluorescence quenching: mechanism and effectiveness in protecting plants from photodamage. *Plant Physiology*. 2016; 170: 1903–1916. <https://doi.org/10.1104/pp.15.01935>

Santrucek J, Sage RF. Acclimation of stomatal conductance to a CO<sub>2</sub>-enriched atmosphere and elevated temperature in *Chenopodium album*. *Australian Journal of Plant Physiology*. 1996; 23: 467-478. <https://doi.org/10.1071/PP9960467>

Seneweera S, Aben S, Basra AS, Jones B, Conroy JP. Involvement of ethylene in the morphological and developmental response of rice to elevated atmospheric CO<sub>2</sub> concentrations. *Plant Growth Regulation*. 2003; 39: 143–153. <https://doi.org/10.1023/A:1022525918305>

Silveira AMF, Coelho Netto RA, Marengo RA. Biomass allocation in *Ceiba pentandra* (Malvaceae) under water stress and high CO<sub>2</sub> concentration. *Scientia Forestalis*. 2023; 51: e3955. <https://doi.org/10.18671/scifor.v51.10>

Vanitha PA, Vijayaraghavareddy P, Uttarkar A, Dawane A, Sujitha D, Ashwin V, et al. Novel small molecules targeting bZIP23 TF improve stomatal conductance and photosynthesis under mild drought stress by regulating ABA. *FEBS Journal*. 2022; 289: 6058–6077. <https://doi.org/10.1111/febs.16461>

Wang Z, Wang C. Responses of tree leaf gas exchange to elevated CO<sub>2</sub> combined with changes in temperature and water availability: A global synthesis. *Global Ecology and Biogeography*. 2021; 30: 2500-2512. <https://doi.org/10.1111/geb.13394>

Way DA, Oren R, Kroner Y. The space-time continuum: the effects of elevated CO<sub>2</sub> and temperature on trees and the importance of scaling. *Plant Cell Environment*. 2015; 38: 991-1007. <https://doi.org/10.1111/pce.12527>

Yang PM, Huang QC, Qin GY, et al. Different drought-stress responses in photosynthesis and reactive oxygen metabolism between autotetraploid and diploid rice. *Photosynthetica*. 2014; 52: 193-202. <https://doi.org/10.1007/s11099-014-0020-2>